



The global island species–area relationship for plants

Thomas J. Matthews^{a,b,c}, Julian Schrader^{d,1}, François Rigal^{c,e}, Kostas A. Triantis^f, Holger Kreft^g, Patrick Weigelt^h, and Robert J. Whittaker^{i,j,1}

Affiliations are included on p. 9.

Edited by Robert Holt, University of Florida, Gainesville, FL; received July 16, 2025; accepted December 23, 2025

The island species–area relationship (ISAR) is known to be near-ubiquitous, but its properties across the fullest span of island areas globally and how island endemism shapes the ISAR remain poorly understood. We determine the global ISAR for native (Nat_{Rich}) and for single-island endemic richness (SIE_{Rich}) of vascular plants, employing data for 1,262 islands, spanning 60.7S to 80.7 N and ten orders of magnitude in area. Using logged species number and area, we compared the power model and four different breakpoint models. For Nat_{Rich} , a simple power model (slope, $z = 0.32$, $R^2 = 66\%$) was best supported. For SIE_{Rich} , a flat-steep breakpoint model outperforms the power model, with the latter producing a steeper slope ($z = 0.48$, $R^2 = 0.47$) than for Nat_{Rich} . Rerunning the Nat_{Rich} power model for subsets of islands of increasing endemism generates increased ISAR slope and improved prediction of continental richness values. Controlling for island area, Nat_{Rich} declines with isolation, while endemism increases. Semilog analyses show that old, tropical, mountainous continental fragments and landbridge islands, rich in SIE, drive an accelerated increase in Nat_{Rich} for islands $>10,000 \text{ km}^2$ in size. The global Nat_{Rich} archipelago species–area relationship was best described by a power model ($z = 0.41$, $R^2 = 0.54$), and there is also evidence of declining richness but higher endemism with increased archipelago isolation. Our findings provide no support for the existence of an upper asymptote in the global plants ISAR, while supporting the application of the power model at a global scale, and highlighting roles for island type, endemism, and isolation as influences on ISAR form.

island biogeography | island endemism | plant diversity | power model | species–area relationship

Ecologists and biogeographers have long been interested in describing and explaining the species–area relationship (SAR), the general pattern whereby the number of species increases with the area considered (1, 2). A large body of theory has built up concerning SARs, with important applications, for example, in conservation science (3–5). Rather than a single pattern, however, there are actually several distinct ways and contexts in which SARs may be constructed—and their mathematical properties differ (1, 6). The most important distinction is between: i) those that are species-accumulation curves (nested species–area relationships, e.g., ref. 7) and ii) those fitted for noncumulative totals, typically island species–area relationships, or ISARs (8). Here we are concerned solely with the properties of ISARs, by which we refer to the mathematical form of best-fit models of the number of species occurring within each of a set of islands as a function of the area of each island.

Islands are important both as model systems in biogeography and for their disproportionate contribution to global biodiversity (9), and ISARs are a key tool for understanding how they do so (2, 10). While more complete explanatory models for island species diversity can be constructed by inclusion of additional variables alongside area (e.g., refs. 11 and 12), it is of long-standing theoretical interest to determine the form taken by the ISAR (1, 13, 14). Should a single model be found to describe the ISAR that is broadly consistent in its parameters across study systems and range in area and insular context globally, then it may be inferred that the biological processes shaping it must be both powerful and general. The emergence of predictable departures from such a simple scenario can indicate scale and/or context dependence and again may be biologically informative (2, 8, 10, 15). Island biogeographic theory posits that increase in island area permits both greater habitat diversity (providing for more distinct niches) and larger populations (greater carrying capacity, reducing extinction rate), and with still greater area, the subdivision of habitats also typically increases (e.g. through mountains forming internal barriers), but area alone is almost never sufficient to explain variation in richness in its entirety (1, 8, 10, 12, 13). Geographical isolation, which limits colonization opportunities, and climate variation, which influences carrying capacity, are typically the first additional variables considered in more complete multivariate models (11–13). Isolation is of particular biogeographical significance, as it limits the rate of propagule exchange, leading to depressed immigration rates, lower turnover rates, and thus increasing

Significance

The increase of species richness with island area—the island species–area relationship (ISAR)—is considered an ecological law, although its precise form remains controversial. For the global vascular plant ISAR (and the equivalent archipelagic relationship), we demonstrate that a simple power model explains a remarkable amount of variation, with ISAR slope and residual variation explicable by isolation, island origins, and proportion of endemism. Increased isolation drives richness down, only partially compensated for, as area increases, by in situ speciation. Large, tropical, mountainous islands that were also formerly connected to continents are both rich in endemics and exceptionally species-rich overall. When extrapolated, our all-islands ISAR underestimates continental richness values, showing no evidence of an asymptote in the global SAR.

Author contributions: T.J.M., J.S., F.R., K.A.T., H.K., P.W., and R.J.W. designed research; T.J.M. and F.R. analyzed data; and T.J.M., J.S., and R.J.W. wrote the paper.

The authors declare no competing interest.

This article is a PNAS Direct Submission.

Copyright © 2026 the Author(s). Published by PNAS. This article is distributed under Creative Commons Attribution-NonCommercial-NoDerivatives License 4.0 (CC BY-NC-ND).

PNAS policy is to publish maps as provided by the authors.

¹To whom correspondence may be addressed. Email: jschrader@posteo.de or robert.whittaker@ouce.ox.ac.uk.

This article contains supporting information online at <https://www.pnas.org/lookup/suppl/doi:10.1073/pnas.2518902123/-/DCSupplemental>.

Published February 17, 2026.

opportunities for in situ speciation, whether by cladogenesis (in situ lineage division leading to two or more new species through adaptive or nonadaptive evolutionary changes) or anagenesis (evolutionary change arising between an island population and the source pool) (10, 13, 14).

Numerous studies have examined the properties of ISARs constructed at the level of individual island groups/archipelagos (e.g., refs. 4, 8, 16, and 17). Building on a previous analysis of 488 island floras (12), we set out to describe, using a wide range of model types, the ISAR form for a globally distributed set of >1,200 islands spanning the full range of island area, degrees of isolation, and different marine island types, using data for vascular plants. This expanded data coverage allows us to test for consistency of the shape of the ISAR from the smallest to the largest spatial scales and for how island endemism contributes to it across the world's islands.

The oldest and simplest models proposed to describe ISARs are i) the power model, $S = cA^z$, (eqn 1), and ii) the logarithmic model, $S = c + d \log A$, (eqn 2), where S is species number, A is area, and c , z , and d are fitted parameters (1, 16). Comparative analyses of the performance of 20 mathematical models of varying complexity, fitted to several hundred datasets for island groups, have established that the power model provides the best general solution (8, 18). For analytical and graphical expedience, the power model is generally fitted using linear regression following log-transformation of both area and species number as $\log S = \log c + z \log A$, which we can call the log-power model variant (eqn 3). This is the dominant implementation of the power model and it generates two mathematically independent constants, the slope z (the rate at which richness increases with area) and the intercept $\log c$ (the log-transformed richness of an island of unit area), which permit biogeographical inference in comparative analyses (4, 16, 19, 20). Hence, the two dominant analytical approaches to fitting ISARs involve: (i) logging both area and species richness (as per eqn 3), and (ii) logging area only (as per eqn 2). We employ both strategies herein: the specific models used are described below (see Materials and Methods).

There have been numerous theoretical contributions to understanding ISAR scale dependency, of which Rosenzweig's scale-structured SAR model (2; Fig 9.11) is of seminal importance. Rosenzweig's model suggests three to four scales of diversity variation, two of which apply to ISARs. He argues that when log-power ISAR models are fitted to data from islands within archipelagos, lower slopes are obtained ($z = 0.23 - 0.33$) than for data derived from provinces ($z = c. 0.9$). Provinces for these purposes are biogeographical areas that largely generate their own species by in situ cladogenesis rather than by immigration from other areas. Following this reasoning, it is possible to consider oceanic islands and archipelagos that are geographically isolated and rich in endemics to be province-like systems (21, 22). In a similar vein, others have predicted that beyond a certain threshold of island area, at which in situ cladogenesis becomes important as a contribution to island diversity, the rate of gain of richness with increased area accelerates, leading to an increase in the ISAR slope (15). Some support for these theoretical arguments comes from two lines of evidence: (i) ISARs for endemics of oceanic islands are systematically steeper than those for nonendemic natives of the same island systems (21) and (ii) fits for archipelago species-area relationship (ASARs, whereby each data point is for an archipelago) show steeper slopes than typical of the ISARs of their constituent islands (2, 14, 22). Further support comes from studies showing that, beyond a certain threshold area, speciation contributes a high proportion of species richness to island systems, leading to ISARs that are not only steeper, but sometimes may be

better described by two-phase ("flat-steep") breakpoint models (23–25). In contrast, suggestions of an upper-asymptote, a flattening toward the right-hand end of the ISAR (15) have proven controversial (26, 27) and appear to lack empirical support (8).

Although archipelago-scale ISARs have been subject to detailed scrutiny, the form taken by ISARs and ASARs across the full global range of island area, and how speciation influences their parameters at this scale, have not. Based on the foregoing, we hypothesize that once islands are large enough for in situ cladogenesis to contribute meaningfully to overall island richness, the rate of gain in species number with area accelerates (2, 15). Long-established biogeographical theory and observation also predict that this pattern should be most apparent in more productive climate regimes, such as pertains for low-latitude tropical island systems (e.g., ref. 28).

Hence, our first goal in this paper is to describe the form taken by the global ISAR spanning from the smallest to the largest islands. We use native vascular plants as our model system as a) they are an important, generally diverse, component of all island ecosystems across the globe, b) they are generally less severely influenced by anthropogenic extinctions compared to other well-studied taxa, and c) there are good data available for a full range of island areas and also for continents, allowing ISAR form to be placed in a broader context (9). Herein, i) we explore the form of the global ISAR using a range of data transformations and models, including breakpoint models capable of detecting rate changes in the response to area and models that incorporate spatial structure; focusing specifically on the log-power model, we then ii) describe the global ISAR and its relationship to continental species richness variation; iii) explore how variation in ISAR form relates to island isolation, island type, and proportion of endemism within the flora; and finally, iv) we describe the form of the global ASAR. A schematic of our analytical pipeline is provided as *SI Appendix, Fig. S1*.

Results

We compiled data for 1,262 islands ("All islands," Table 1), ranging in area by ten orders of magnitude from 0.000018 km² to 816,018 km² (New Guinea) and in species richness from 1 to 12,647 (Fig. 1, *SI Appendix, Fig. S2*, and *Dataset S1*). The islands range from 60.7S to 80.7N and include a mix of continental shelf (Pleistocene land-bridge) islands, ancient continental fragments, atolls, and volcanic oceanic islands. Following the global size distribution (10), the islands in our dataset are heavily skewed toward small islands: 624 are <1 km² in area, and a further 200 are of 1 km² to 10 km², with just 13 exceeding 100,000 km² (*SI Appendix, Fig. S2*).

Global ISAR Model Fitting and Comparison. In the comparison of simple and breakpoint power models in log-log space, the best fit for the global ISAR for native plant species richness (Nat_{Rich}) is provided by the log-power model (a simple linear fit in Fig. 1A), which explains 66% of the variation, with slope, z of 0.32 ($SE = 0.01$) (Tables 1 and 2 and *SI Appendix, Table S1*). The global Nat_{Rich} ISAR, if extrapolated, underpredicts continental richness (by 75% on average when predictions are first transformed to the raw scale). The largest islands display both positive residuals and high proportions of endemism. As very small islands support few single-island endemics (SIEs) (Fig. 1A and B), the best fit model in log-log space for SIE_{Rich} is a two-phase flat-steep breakpoint model ($R^2 = 51\%$), with the breakpoint occurring at 78 km² (Fig. 1B and Table 2). The simple log-power model explains only slightly less variation ($R^2 = 47\%$, $z = 0.48$ [$SE = 0.03$]) and generates an area threshold of 3.35 km² below which islands generally lack SIE (Table 1). Extrapolation of both SIE_{Rich} ISARs in Fig. 1B shows

Table 1. Parameters and performance of the global ISARs for vascular plants according to the log-power model

Island and species selection	N	z	logC	R ²	Island size (km ²) where richness = 1
All islands: Nat _{Rich}	1,262	0.32	1.72	0.66	<0.0001
Islands with SIE: SIE _{Rich}	244	0.48	-0.25	0.47	3.35
Islands with >5% SIE: Nat _{Rich}	75	0.44	1.36	0.83	<0.001
Oceanic islands: Nat _{Rich}	704	0.31	1.66	0.53	<0.0001
Oceanic islands with SIE: SIE _{Rich}	178	0.34	0.04	0.21	0.77

Nat_{Rich} = native plant species richness; SIE_{Rich} = single island endemic richness. The island area threshold where Nat_{Rich} or SIE_{Rich} = 1 is, in each case, obtained from the relevant log-power model. Note that islands with zero SIE_{Rich} were excluded from the SIE_{Rich} analyses. In addition to the all islands analyses, we have included values for the Nat_{Rich} analysis using islands of >5% SIE and the Nat_{Rich} and SIE_{Rich} analyses for oceanic islands. N = number of data points.

that they again underpredict the endemic richness of continents, although less so in the case of the breakpoint model. Islands with a higher percentage of endemic species again appear to contribute

disproportionately to positive model residuals, especially the largest islands (Spearman's correlation between residual values [from the log-power model] and percentage endemism: rho = 0.81,

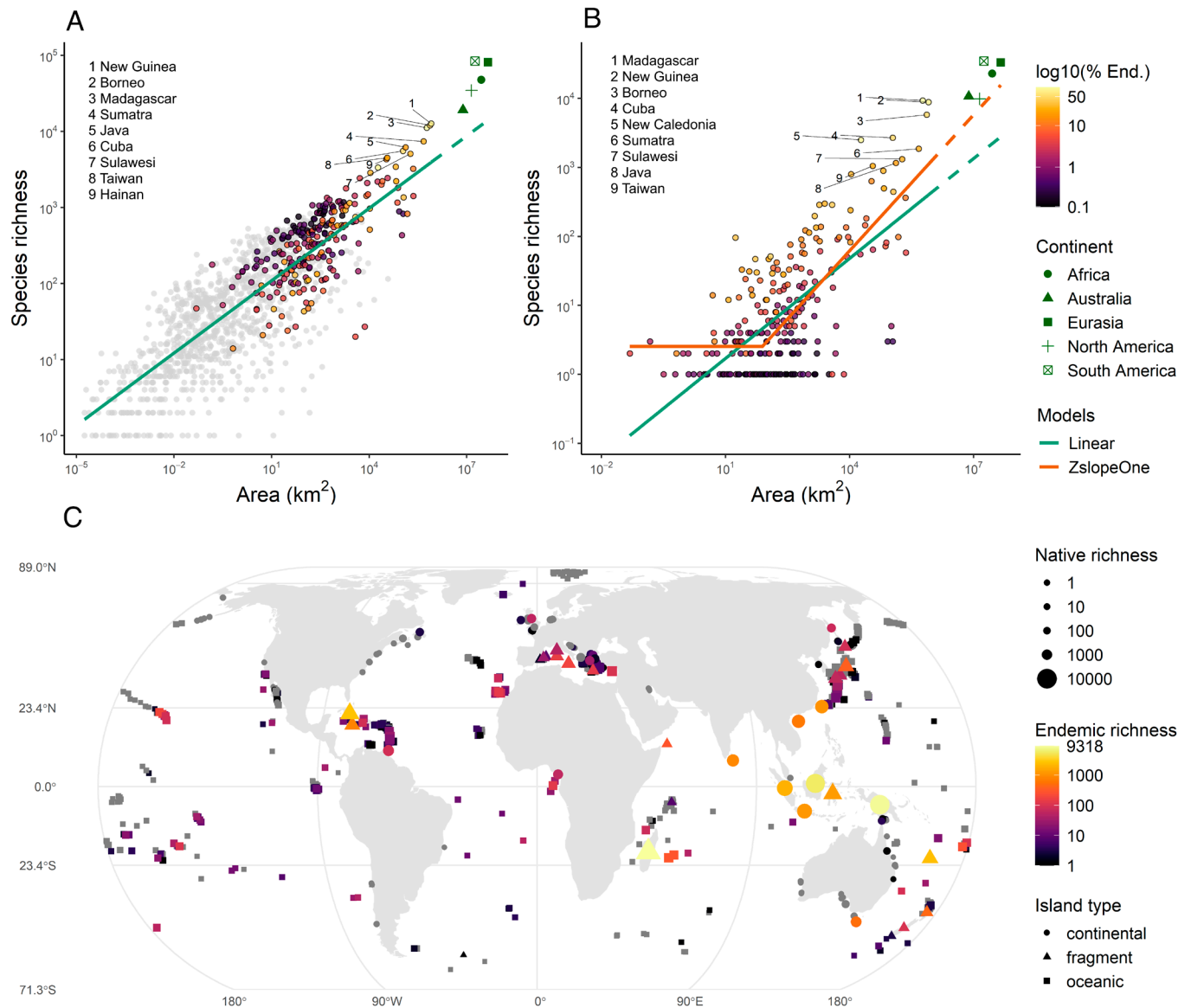


Fig. 1. Island plant species richness. The global island species–area relationship for (A) all native species (number of islands = 1,262) and (B) single-island endemics (number of islands = 244). Within (A), islands with zero endemics are shown as gray circles, but within (B), these islands are excluded from analysis. In both panels, the color shading indicates the percentage of total richness represented by single-island endemics (log-transformed for visualization purposes). In (A and B), the green line represents the fit of the standard log-power model, which in (A) provided a better fit than the breakpoint models (based on BIC), while in (B) a breakpoint (flat-steep) model (brown lines) provides the best fit (Table 2). In both panels, the ISARs are extrapolated to the size of the largest continent for comparative purposes, but the continents are not included in the models (log-power models fitted separately for the five continents (only) were nonsignificant). In (A and B) the names of the nine most species-rich islands are listed. (C) A map of the analyzed islands, with point size representing native species richness and color shading representing single island endemic richness (gray represents islands with no single island endemics). Shape type represents island type: continental shelf islands (continental), ancient continental fragments (fragment), and oceanic islands, i.e., atolls and volcanic oceanic islands (oceanic). Values for continents in (A and B) represent richness of species and of endemic species, respectively.

Table 2. Global plant ISAR model comparison results for log-log space (both Nat_{Rich} and SIE_{Rich})

Model	BIC	R^2	Th1	Th2
Nat_{Rich}				
Linear	1,662.38	0.66	-	-
ZslopeOne	1,669.46	0.66	0.00003	-
ContOne	1,672.51	0.66	229,615	-
ZslopeTwo	1,674.90	0.66	0.0004	0.01
ContTwo	1,676.70	0.66	3,639	3,811
Intercept	3,001.11	0.00	-	-
SIE_{Rich}				
ZslopeOne	490.19	0.51	78	-
ContOne	491.53	0.52	411	-
ZslopeTwo	493.45	0.52	49	225,944
ContTwo	496.04	0.53	216	225,944
Linear	504.76	0.47	-	-
Intercept	652.54	0.00	-	-

Th1 and Th2 refer to the values (km^2 , backtransformed from the \log_{10} values) of the breakpoints in the threshold model fits. “ZslopeOne” and “ZslopeTwo” correspond to the zero-slope one-threshold and zero-slope two-threshold models, respectively, while “ContOne” and “ContTwo” correspond to the continuous one threshold and continuous two threshold models. The “Linear” model is the log-power model and the “Intercept” model is an intercept-only null model. The symbol “-” indicates that the calculation of the corresponding value does not apply.

$P < 0.001$). For both Nat_{Rich} and SIE_{Rich} , the fit of the log-power model is robust to the inclusion of spatial structure and archipelago effects in the model (SI Appendix, Fig. S3 and Table S1). For example, for Nat_{Rich} , the z -values of a spatial autoregressive model and a spatial mixed effects model (with archipelago as a random intercept and slope) are 0.33 (SE = 0.01) and 0.34 (SE = 0.01), respectively ($P < 0.001$ in both cases), compared to 0.32 in the standard log-power model ($P < 0.001$). Moreover, when included in either a standard linear model, a spatial model, or a mixed model with \log_{10} isolation, \log_{10} elevation, and absolute latitude as covariates, the effect of \log_{10} area remains positive and highly significant, although the z -values decrease slightly. For instance, in the standard linear model with these three covariates, the z -value for area decreases to 0.26 (SE = 0.01) (SI Appendix, Fig. S3 and Table S1).

Fig. 1 shows that a relatively small number of the largest islands of high endemism are underestimated by the global ISAR using the log-power model. This can be seen more clearly by inspecting the fit of a negative binomial GLM in semilog space for Nat_{Rich} (Fig. 2). This model (coefficient for area = 0.73; SE = 0.01; intercept = 4.4; $P < 0.001$), which also explains a large amount of the variation in richness with just area as a predictor (Nagelkerke pseudo- $R^2 = 0.96$, Efron’s $R^2 = 0.67$, Cox & Snell $R^2 = 0.93$; Fig. 2), demonstrates a strong upswing in the rate of gain of species across the largest islands. It is also worth noting that the fit of this model is very similar to the fit of the standard power model (eqn. 1) in semilog space (SI Appendix, Fig. S4), providing further evidence that the global ISAR of plants is generally well characterized by a power function. As can be seen from Fig. 2, the pronounced increase in the rate of gain of richness with area toward the right-hand end of the distribution is entirely attributable to islands $>10,000 \text{ km}^2$, of which there are 30 (13 continental fragments, 12 continental shelf islands, 5 oceanic islands). The richest 20 of these islands can be characterized as exceptionally large, predominantly old, continental fragments or continental shelf (landbridge) islands, mountainous, and tropical: none are oceanic. We therefore undertook further analyses (below) to tease out the contribution of endemism, island origins, and isolation to ISAR form.

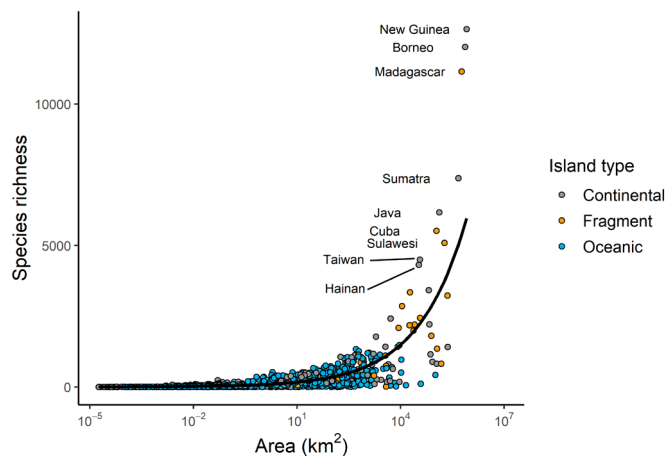


Fig. 2. The fit of a negative binomial GLM (black line) of Nat_{Rich} as a function of \log_{10} area (Nagelkerke $R^2 = 0.96$, slope = 0.73, $P < 0.001$). Data points represent individual islands ($N = 1,262$) and are colored according to the three main island types considered here: continental shelf islands (Continental), ancient continental fragments (Fragment), and oceanic islands (atolls and volcanic oceanic islands; Oceanic). The names of the nine most species-rich islands are shown.

The negative binomial GLM also provided a good fit for SIE_{Rich} in semilog space (coefficient for area = 1.31; SE = 0.07; $P < 0.001$; intercept = -0.1 ; Nagelkerke pseudo- $R^2 = 0.95$, Efron’s $R^2 = 0.39$, Cox & Snell $R^2 = 0.92$; SI Appendix, Fig. S5). The effect of area in the GLMs was robust to the inclusion of spatial structure, with the mean of the posterior distribution of the area coefficient from a Bayesian hierarchical spatial random fields model being 0.73 for Nat_{Rich} (95% credible interval = 0.70–0.76) and 1.31 for SIE_{Rich} (95% credible interval = 1.20–1.43).

The Effect of Island Isolation and Endemism on the Global ISAR.

Island biogeographic theory predicts that having accounted for area, species richness should decrease, and the proportion of endemism should increase with increasing island isolation from mainland source pools (10, 13). The first prediction is confirmed by partial regression analysis of Nat_{Rich} based on island area and isolation (both \log_{10} transformed), as there is a general decrease in richness with increasing isolation after accounting for the effect of island area (Fig. 3A). In addition, when assessing the same relationship for SIE_{Rich} , accounting for area: i) SIE richness tends to increase with isolation, although with much variation; and ii) for any given degree of isolation, there is a trend of residuals switching from negative to positive with increasing proportion of endemism in the flora (Fig. 3B). For Nat_{Rich} , the effect of isolation is similar when \log_{10} isolation is included in either a standard linear model, a spatial model, or a mixed model with \log_{10} area, including models with \log_{10} elevation and absolute latitude as covariates (SI Appendix, Table S1). For SIE_{Rich} , the effect of isolation became nonsignificant in the models that included \log_{10} elevation and absolute latitude (SI Appendix, Table S1).

We further explore the contribution of endemism to Nat_{Rich} ISAR form by progressively restricting the islands included in the ISAR analysis to higher proportions of SIE species per island (Fig. 4). These analyses show that as the %SIE threshold for inclusion in the analysis is increased: i) mean island area continually increases (initially very rapidly); ii) z increases swiftly from 0.32 for all islands to 0.44 for those with $>5\%$ SIE (Table 1), thereafter increasingly only slightly to ~ 0.48 as the threshold is increased to $>25\%$ SIE (Fig. 4); iii) the respective R^2 values are 0.66, 0.83, and 0.91; and iv) extrapolation of the $>5\%$ SIE threshold model results

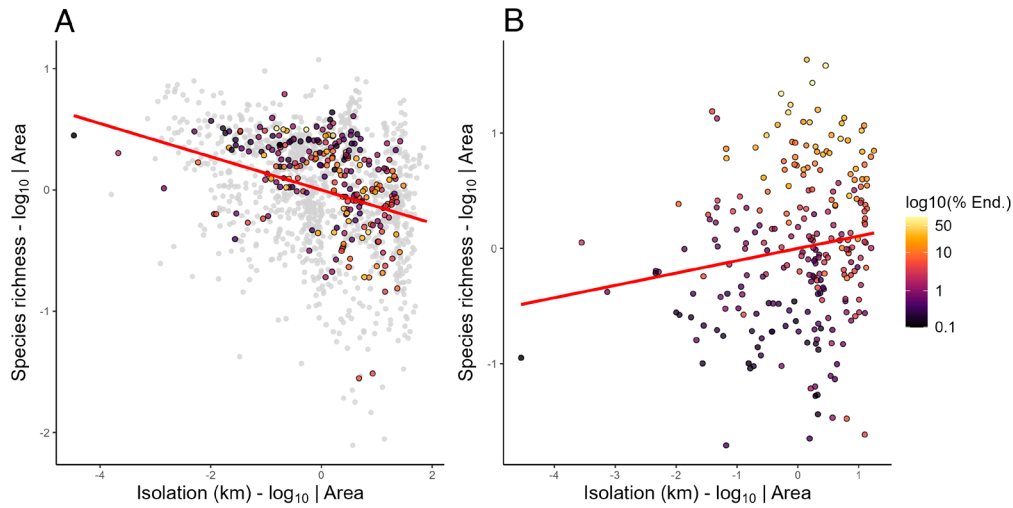


Fig. 3. Partial regression plots showing the relationship between island isolation and richness after accounting for the effect of island area. (A) is for Nat_{Rich} (all native species; number of islands = 1,262), (B) is for single island endemics (number of islands = 244). Points are colored by percentage endemism (log-transformed): islands with no endemics are shown in gray in panel A; these islands are excluded from panel B. The solid lines are the fit of a standard linear regression model (slope = -0.14 , $P < 0.001$ in panel A; slope = 0.11 , $P = 0.02$ in panel B). Isolation and area were log-transformed in all models.

in more realistic predicted continental values (down from a mean of 75% underprediction to an average of 27% different from the observed values).

Oceanic Islands. As island origins and past connections to the mainland can confound inferences, we repeated our primary analyses but for oceanic islands only, i.e., those islands never

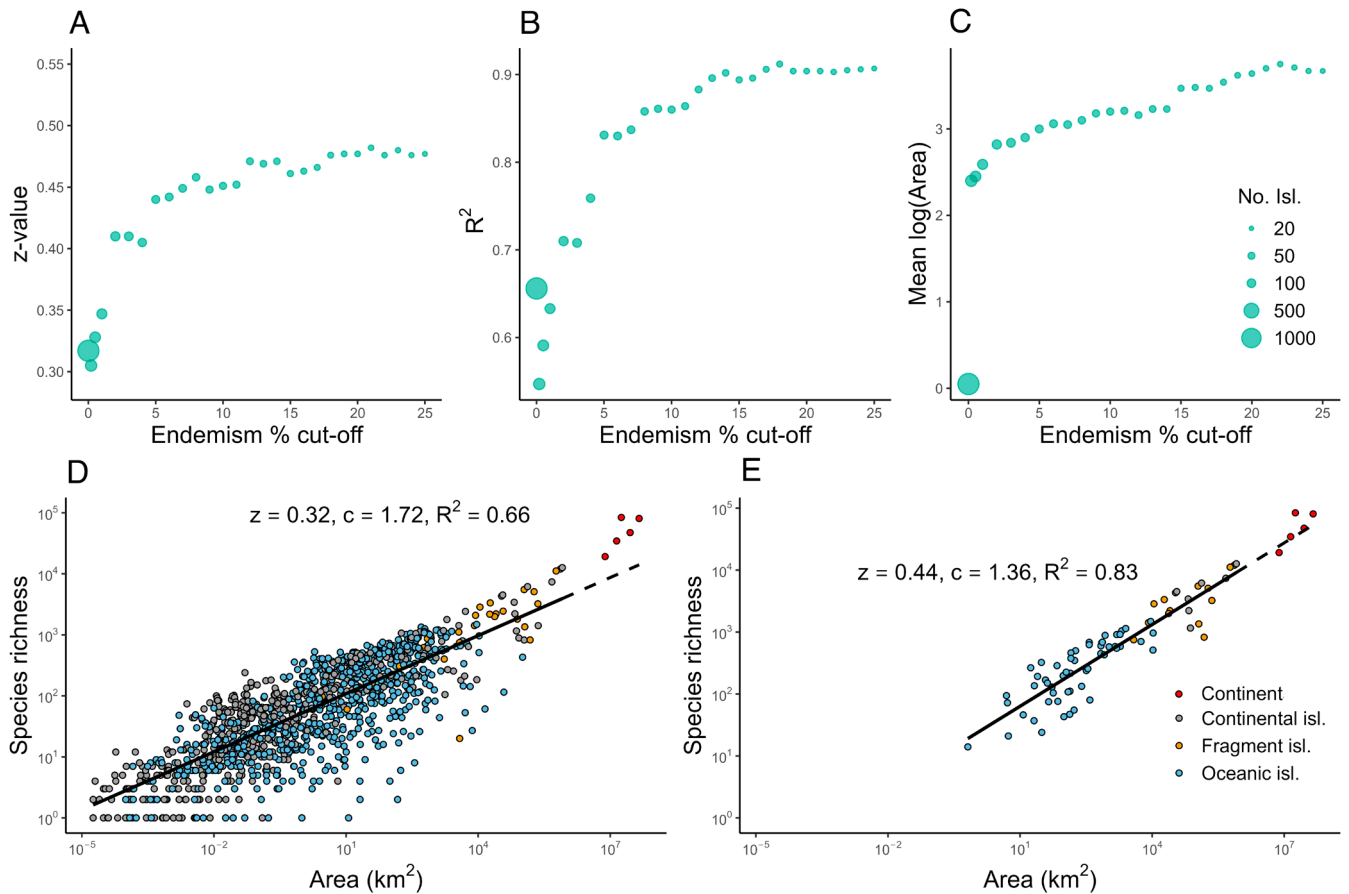


Fig. 4. Change in properties of the global plants Nat_{Rich} ISAR as a function of applying an increasing minimum %SIE threshold for inclusion of islands in the analysis. When the endemism % cut-off value (x-axis) equals zero, all islands ($n = 1,262$) are included in the model. For cut-off values greater than zero, all islands with a proportion of SIEs less than (or equal to) that number are excluded and the log-power model fitted to this subset of islands. Percentage values used were 0%, 0.2%, 0.5%, and then from 1 to 25% in increments of 1%. Point size in (A–C) is scaled by the number of islands in a given subset. (A–C) show, respectively, how the ISAR z-value, ISAR R^2 , and mean $\log(\text{Area})$ of the islands, change as the endemism cut-off level is increased. (D and E) show the global plants Nat_{Rich} ISAR (black line = fit of the log-power model): (D) showing the fit for all islands ($n = 1,262$ islands) and (E) only including islands with $>5\%$ SIEs ($n = 75$ islands). Panel (D) differs from the version presented in Fig. 1 in that point color indicates island type. NB Although the positions of the continents are plotted in panels (D and E), they were not included in the fitting of the ISARs.

connected to a continent. Restricting the island selection in this way also has the effect of slightly reducing the area range in the dataset (above, *SI Appendix*, Fig. S2). The best statistical model for Nat_{Rich} (model comparison presented in *SI Appendix*, Table S2) was found to be a two-phase breakpoint model showing a steep decline in richness with area over the largest few oceanic islands, which is a consequence of the largest oceanic islands comprising exclusively high latitude systems: Isles Kerguelen, three of the Svalbard islands, East Falkland Island, and Iceland. Given this, coupled with the fact that the better fit of the breakpoint model relative to the linear (log-power) model was negligible ($\Delta\text{BIC} = 0.51$), we set aside this model in favor of the ecologically more parsimonious (log) power model ($R^2 = 0.53$). For SIE_{Rich} , the log-power model provided the best statistical model ($R^2 = 0.21$; *SI Appendix*, Table S2). Focusing on the two log-power models, the SIE_{Rich} ISAR slope ($z = 0.34$ [$\text{SE} = 0.05$]) was once again steeper than the Nat_{Rich} ISAR ($z = 0.31$ [$\text{SE} = 0.01$]), although the difference was less pronounced and the models were of lower explanatory value than the equivalent all islands models (Table 1 and *SI Appendix*, Fig. S6 and Table S2). The proportion of endemics does not appear to have a clear role in explaining residual variation in Nat_{Rich} (*SI Appendix*, Fig. S6; Spearman's correlation between residual values and percentage endemism: $\rho = 0.07$, $P = 0.08$), but for SIE_{Rich} (*SI Appendix*, Fig. S6; $\rho = 0.84$, $P < 0.001$), islands with high levels of endemism are dominant among the islands showing positive residuals. The log-power models for both Nat_{Rich} and SIE_{Rich} , when extrapolated, as for the all-island types analyses, underpredict continental richness, while applying a threshold for inclusion of $>5\%$ SIE shows that predicted values for continents are of the right order of magnitude (Figs. 1 and 4 and *SI Appendix*, Figs. S6 and S7). The results of partial regression analyses including isolation and the analyses subdividing the dataset based on the proportion of SIEs were very similar to the all-islands equivalents (Fig. 3 and *SI Appendix*, Figs. S7 and S8). As in the all-island analyses, the fit of the log-power model was relatively robust to the inclusion of spatial structure and archipelago effects (*SI Appendix*, Fig. S9 and Table S3), although the z -values (i.e., area coefficients) were slightly larger and there was a more pronounced difference between the SIE_{Rich} ($z = 0.43$ [$\text{SE} = 0.06$]) and Nat_{Rich} ($z = 0.35$ [$\text{SE} = 0.02$]) ISARs when fitting a mixed-effects model (with archipelago as a

random intercept and slope). When incorporated into either a standard linear model, a spatial model, or a mixed model, including models that also included \log_{10} elevation and absolute latitude as covariates, the effect of \log_{10} area and \log_{10} isolation were relatively similar, although the effect of isolation became nonsignificant in some of the spatial and mixed models (*SI Appendix*, Table S3).

The Global ASAR. Finally, we report the global Nat_{Rich} ASAR, for which the best model was the log-power model (Fig. 5A and *SI Appendix*, Table S4). The slope for the Nat_{Rich} ASAR ($z = 0.41$ [$\text{SE} = 0.03$]; $R^2 = 0.54$) is steeper than for the Nat_{Rich} ISAR ($z = 0.32$). Archipelagos lacking archipelagic endemics tend to be small. Larger archipelagos possessing the highest proportion of archipelagic endemics appear to contribute disproportionately to positive ASAR residuals (Fig. 5A). There is a general decrease in richness with increasing isolation after accounting for the effect of archipelago area (near-continent archipelagos generally have positive residuals, remote archipelagos mostly provide negative residuals), a pattern which appears linked to the proportion of endemics held by each archipelago (Fig. 5B). The best model for the global Archipelago-Endemics $_{\text{Rich}}$ ASAR was a linear model ($z = 0.37$ [$\text{SE} = 0.07$]; $R^2 = 0.23$), while partial regression showed no trend in richness with isolation after accounting for area (*SI Appendix*, Figs. S10 and S11 and Table S4). The z -values of the log-power ASAR models were relatively robust to the inclusion of spatial structure (*SI Appendix*, Table S5), but spatial correlograms indicated that the spatial autoregressive error models did not fully remove the spatial autocorrelation in the model residuals (*SI Appendix*, Fig. S12). On the whole, the effect of \log_{10} area and \log_{10} isolation did not differ substantially when incorporated into either a standard linear model or a spatial model, including models that also included \log_{10} elevation and latitude as covariates, although the effect of area was lower for Endemics $_{\text{Rich}}$ (~ 0.25 vs. ~ 0.40 for the models with just area as a predictor) when included in models with \log_{10} isolation, \log_{10} elevation, and latitude (*SI Appendix*, Table S5).

Overall, the diagnostics conducted for all fitted models did not reveal any notable deviations from statistical assumptions other than those stated above. Plots of residuals vs. fitted values and residual distributions for the various models described above are provided in *SI Appendix*, Figs. S13–S30.

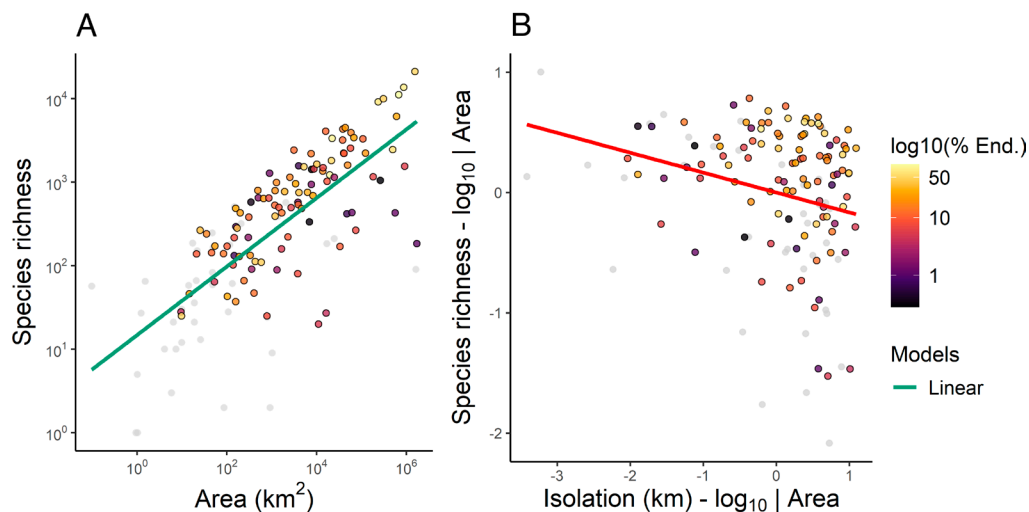


Fig. 5. Vascular plant richness for the world's archipelagos. (A) the archipelago species–area relationship (ASAR) ($n = 139$, slope = 0.41, $P < 0.001$, $R^2 = 0.54$); the green line represents the fit of the standard log-power model, which provided a better fit than the breakpoint models (based on BIC). (B) Partial regression plot showing the relationship between archipelago isolation and richness after accounting for the effect of archipelago area ($n = 139$, Slope = -0.17 , $P < 0.001$, $R^2 = 0.07$). The shading of points represents the proportion of the flora endemic to each archipelago and points shown in gray are for archipelagos without endemics. Isolation and area were log-transformed in all models.

Discussion

'Where speciation is important, as in large islands and continents, the expected size of the fauna is exceeded, but the relationship between area and the size of the fauna is not lost, but accentuated.' Source: Munroe (29); also cited by Lomolino (15).

We set out to provide a detailed evaluation of the form of the global ISAR for vascular plants, with additional analyses for oceanic islands, for single-island endemics, and for the global ASAR. The NAT_{Rich} ISAR slope (z) of 0.32 for all 1,262 islands is consistent with that estimated from an earlier study of just 488 islands ($z = 0.31$) (12), indicating that the global ISAR for plants is a robust biogeographic pattern. It is remarkable that 66% of the variation in global insular plant richness can be explained by area alone, providing further support for the SAR as an ecological law and attesting to the generality of the power model as a tool for describing ISARs across a wide range of scales and contexts (1–4, 7, 8, 12).

We were particularly interested in testing for the increase in rate of gain on larger islands, previously hypothesized (2, 15, 29) as a likely outcome of the increased importance of speciation. Interestingly, we found that the equivalent log-power model for SIE_{Rich} is much steeper ($z = 0.48$) than that for all native species. Moreover, a breakpoint model with a flat phase followed by a still steeper phase for larger islands was found to provide a better fit for SIE_{Rich} than the log-power model. All else being equal, the importance of speciation as a source of species within an island is expected to scale positively with island area for several reasons. First, a larger island provides more opportunities for within-island geographic isolation of populations and subsequent allopatric divergence and, ultimately, speciation (2). Second, larger islands typically contain a greater range and diversity of habitats (30), which may strengthen selective pressures and result in increased rates of evolution of reproductive isolation (25). Finally, larger islands also typically support larger population sizes (13). Larger populations are less likely to go extinct and thus are more likely to survive long enough to undergo speciation, as well as being more likely to be subdivided into allopatric populations (25).

The greater rate of within-island speciation on larger islands has previously been shown to steepen the ISAR for individual archipelagos (e.g., refs. 23–25) but here we find evidence for similar patterns at the global scale. For both NAT_{Rich} and SIE_{Rich} , the very largest islands are underfitted by our All islands models (i.e., they have considerably more species than indicated by the model fit). These islands are all either continental shelf (land bridge) or continental fragment islands of complex topography situated in tropical latitudes (Fig. 1). The significance of these islands to global ISAR form can be seen most starkly when fitting the data with a negative binomial GLM in a semilog space (Fig. 2). Indeed, the predicted curve shows a strong upward swing for the largest islands, while still underfitting them. More broadly, these results necessitate further analyses and theory building in order to better understand the extent to which speciation on larger islands only partially compensates for the reduced immigration inherent to being an island, fully compensates, or overcompensates. Within such analyses, it will be important to distinguish between allopatric replacements and cladogenesis within the island of interest, as well as instances of persistence of paleo-endemics, especially for some of the oldest tropical, continental islands (14).

Our subsidiary analyses demonstrate several phenomena that are expected from island theory. For instance, there is a threshold island size below which islands generally lack their own endemic plant species, estimated via the power model ISARs at 0.77 km²

for oceanic islands and 3.35 km² for all islands. These values are considerably smaller than the 14.6 to 107.8 km² previously estimated for vascular plants by Kisel and Barraclough (31), but this is unsurprising because theirs was a minimum threshold for in situ cladogenesis, a process which on theoretical grounds we should expect to require a larger land area than merely for an island to be capable of supporting an endemic that may have arisen allopatrically and by anagenesis. Indeed, even within birds, the recently split Wilkins's bunting (*Nesospiza wilkinsi*) is endemic to Nightingale Island (32), which coincidentally is not greatly different in size (~3.2 km²) to the threshold size we have observed for plants and is an example of anagenesis. There are also birds endemic to smaller islands (e.g., the Nihoa finch, *Telespiza ultima*, currently endemic to the 0.69 km² island of Nihoa), but their restricted distributions are believed to be relictual and the result of anthropogenic extirpations from larger islands nearby.

Given that our selection of islands spans the globe and thus includes great variation in climate regime and island types, it is remarkable how much of the variation in insular plant richness can be explained simply by island area (66 to 96% for NAT_{Rich} , depending on the chosen model and R² formulas). As such, these results provide further evidence of the extraordinary importance of area (i.e., size of island and those other properties that scale with it) in island biogeography (2, 8, 15). Of the residual variation, our analyses indicate that isolation from mainlands can account for a significant amount of it. For NAT_{Rich} , we observe a decrease in richness with increasing isolation (Fig. 3A), a theoretically expected pattern given the reduction in colonization rates on islands with increasing distance from the mainland (13, 33). In contrast, for SIE_{Rich} , there is an increase in richness with isolation as well as a general tendency for more positive residuals from this relationship with increasing degree of endemism (Fig. 3B). Again, these patterns are predicted by theory as, all else being equal, more isolated islands have reduced gene flow with populations elsewhere, leading to genetic divergence and thus a greater likelihood of speciation (10). Additional predictor variables not included here, such as intra-archipelago isolation (34), climatic factors (11), and island age (14), would likely help explain any remaining residual variation. However, our aim was to study the form of the global ISAR, while also accounting for the known interaction between area and isolation in shaping insular plant diversity (9), rather than to build a full explanatory model of island plant richness (see ref. 12).

Rosenzweig (2) has argued that areas that are large enough to generate and sustain their own species through speciation equate to provinces and that increased provinciality will steepen ISAR slopes (14, 21). Here we show that the ISAR slope (z) does indeed increase as the selection of islands is narrowed by gradually increasing the minimum proportion of SIE species required for inclusion in the calculus. Not only did we find steeper slopes (z increasing from 0.32 to 0.44) and improved fits, but we also found that estimates of continental richness values generated by extrapolation of the ISAR improved markedly as we reduced the selection from all islands up to those of >5% SIE, at which point observed values for North America, Africa, Eurasia, and South America were underpredicted by 7.7%, 8.3%, 33.9%, and 57.7%, respectively, while Australia was overpredicted by 27.5% (Fig. 4E). That is to say, consistent with Rosenzweig's provinciality arguments, and at least for vascular plants, area alone permits the construction of a coherent power model ISAR embracing both islands and continental land masses when basing the calculations on islands possessing a minimum of 5% endemics. While Rosenzweig has previously demonstrated a similar case for fish species, his analysis was based on a dataset of just four islands and three continents (2). Overall, consistent with the arguments of Williamson et al. (26, 27)

and Triantis, Guilhaumon, and Whittaker (8), our analyses provide no support for the hypothesis (e.g., ref. 15) of a gradual leveling of the curve at the right-hand end of the SAR.

We also find that the global ASAR is steeper than the global ISAR, reflecting the importance of within-archipelago speciation in building island floras. As we have conducted these analyses on a global dataset, unlike previous tests of this idea (e.g., ref. 21), our analysis holds the danger of differences in island properties other than area also confounding this analysis. This is reflected in the two-phase breakpoint model for oceanic islands that we dismissed on the grounds that the bias of the largest oceanic islands to high latitudes was dragging down the final phase with increasing area such that it dived downward rather than accelerating upward. The analyses restricted to oceanic islands (albeit comprising a mix of atolls and volcanic islands) are nonetheless useful in constraining the variation in island properties compared to our full dataset. For this oceanic island dataset, it is apparent: i) that increasing proportions of endemism correspond with positive ISAR residuals for SIE_{Rich} , especially so for larger oceanic islands, but that ii) the analyses for NAT_{Rich} provide no support for a change of rate of gain in plant species richness for larger oceanic islands. While the uptick in the rate of gain of species across the largest islands hypothesized by Lomolino (15) is apparent in the semilog plot and negative binomial GLM for NAT_{Rich} in our full (all islands) dataset, it appears attributable to the dominance in the largest size classes of continental fragment and continental shelf islands that are predominantly old, tropical, and mountainous, which begs the question as to what extent their exceptional diversity is a function of their current insularity, or of their high productivity, mountainous terrain, high habitat heterogeneity, large size, age, and complex geodynamic histories (35–37). The extent to which the findings reported herein hold for other taxa is of considerable interest and we therefore intend to address this in a future publication.

Materials and Methods

Species Occurrence Data. We sourced species richness data for native and endemic vascular plant species on islands worldwide from Schrader et al. (9), the most comprehensive assessment of insular plant diversity and endemism to date. This dataset is based on the Global Inventory of Floras and Traits database GIFT v.3.2 (38) and holds information on the status and occurrence of 304,103 species, of which 94,052 occur on 1,651 islands globally. In total, GIFT includes plant inventories from around 3,400 island and mainland regions worldwide, sourced from checklists, floras, and reports, and also including such major species distribution databases as the World Checklist of Vascular Plants (39) and the Integrated Assessment of the Vascular Plant Species of the Americas (40). Based on the full island dataset from Schrader et al. (9) we then further refined it by i) excluding Greenland from the dataset as it is largely ice covered and there is some doubt whether it would be a single island were the ice to be removed, ii) filtering out all islands for which floristic assessments were not considered comprehensive either by the original author(s) or GIFT (342 islands), and iii) removing the single remaining island with zero species. This left 1,307 islands in our dataset. We then removed islands where the data were actually not from a single island but rather were from an archipelago within which the largest island (to which the species list was attributed in GIFT) provided less than 80% of the archipelagic area (e.g., the Bismarck Islands): reducing the dataset to 1,262 islands (Dataset S1). We also extracted from GIFT: i) a separate archipelago-level dataset (Dataset S2: providing the number of species occurring on individual archipelagos globally), and ii) species richness data for continents (included in Dataset S1).

Species numbers were obtained by counting all species native or endemic to each island or archipelago in our dataset. We used the species endemism status for all islands globally following the *expert-based OR exclusion method* outlined in Schrader et al. (9). This dataset lists all species endemic to an island or archipelago that were either i) considered endemic to a specific island or archipelago by the original author(s) of the species checklist or flora (expert-based), or ii)

reported as native to an island or archipelago but absent from any other region in GIFT (exclusion-based). This produced endemism counts at the level of single islands (i.e., SIEs: single-island endemics) that we used for the ISAR analyses, and for single archipelagos, used for the ASAR analyses.

To obtain the species number for each of the five large mainland land masses except Antarctica—North and South America, Eurasia, Africa, and Australia—we constructed species lists for all geographical regions in each of these landmasses from GIFT and derived their respective species numbers. Species lists were organized according to the Botanical Continents (41), which divide the Americas at the southern border of Mexico into Northern and Southern America. Eurasia comprises three Botanical Continents—Europe, Asia-Tropical, and Asia-Temperate—which we combined into a single list for the region. For species endemic to these regions, we used the exclusion method, indicating all species as endemic that did not occur on any other continent or island region. Australia is treated here as a continent rather than an island, following the usual convention in the island biogeographical literature (e.g., ref. 9).

Apomictic taxa—species that reproduce asexually—have evolved independently across various genera (42). Identifying and defining apomixis within species concepts remains a debated issue and the representation of apomicts in GIFT is inconsistent, potentially introducing species richness bias toward well-sampled regions in Europe and North America (43, 44). To mitigate this, we used the dataset from Schrader et al. (9) that excluded apomictic taxa.

Island Area, Isolation, Elevation, and Attribution to an Archipelago. For all islands we sourced their land area, isolation and elevation from the GIFT database. As our isolation metric, we used the distance to the nearest mainland in km. All raw area values are in units of km^2 . We delineated archipelagos following Schrader et al. (9). Islands were grouped by shared geological origin, such as atolls (for example, Maldives), volcanic hotspot chains (for example, Hawai'i, Galápagos), or by geographic proximity and connectivity during the last glacial maximum (for example, continental-shelf archipelagos). Using these criteria, we assigned islands to 108 archipelagos (Dataset S1). For some groups, especially those on continental shelves, boundaries are traditional but partly arbitrary, and some islands could be classified differently. Many archipelagos also contain smaller islands or islets lacking species data; only islands with available data were included in species area totals of their respective archipelagos for the archipelagic dataset (Dataset S2, comprising 139 archipelagos, more than in Dataset S1 because for some archipelagos we lack island-level data).

ISAR Model Fitting and Comparison. The model fitting and comparison was undertaken using two different versions of the main dataset. First, we used the data for all native species on the 1,262 islands (NAT_{Rich}). Second, we focused on just single island endemic species (SIE) and only included the 244 islands with at least one single island endemic (SIE_{Rich}). As the use of log-transformation in ISAR model fitting is known to emphasize different parts of the relationship, we explored the form of the global ISAR in both semilog space (i.e., where area is log-transformed but richness is not) and log-log space. When logging data, log_{10} was used in all cases. To assess the form of the global ISAR in log-log space and test for the presence of any breakpoints in the relationship, we compared the fit of five ISAR models: the log-power model (eqn. 3), and four breakpoint models (two models with a single breakpoint [threshold] and two models with two breakpoints). The breakpoint models were all continuous, and in two models the first segment was fixed to have a slope of zero (zero-slope one-threshold and zero-slope two-threshold models), while in the other two models the slopes of all segments were allowed to vary (continuous one threshold and continuous two threshold models). To avoid model fits with very small numbers of data points in a segment, we set the minimum number of islands to be contained within each of the two segments (in the case of one-threshold models), or the first and last segments (in the case of two-threshold models), to five (45). The models were fit using piecewise regression and the "sar_threshold" function in the "sars" R package [(20), see ref. 45 for further information on fitting the breakpoint models]. The resultant fits were compared using the Bayesian information criterion (BIC), and the model with the lowest BIC value was considered to provide the best fit (46). We used BIC as the penalty on the log-likelihood associated with the number of parameters is stronger, relative to Akaike's information criterion (AIC) and sample size-corrected AIC (AIC_c), with our sample sizes (47), and we wanted to ensure a strong test of threshold fits and reduce the likelihood of overfitting the data. We

considered the search for a breakpoint to represent a free parameter and thus we added one unit per threshold to the original number of model parameters in the breakpoint models (45). The breakpoint search interval was fixed at 0.01 (in units of log area).

To explore the global ISAR in semilog space, we used a different approach to that used in log-log space. To account for overdispersion in the data, we fitted a Type 2 negative binomial (log link) generalized linear model (GLM) with area (log-transformed) as the predictor and richness as the response (48), using the "glm.nb" function in the "MASS" R package. As there is no consensus on the most appropriate measure of R^2 for negative binomial GLMs, we calculated three commonly used R^2 values in this context, namely the Nagelkerke pseudo- R^2 , the Efron R^2 , and the Cox and Snell R^2 , using the "performance" R package (49). For the log-log (log-power model) and semilog space analyses, model evaluation was undertaken through plots of the residuals vs. fitted values and spatial correlograms to identify any potential spatial autocorrelation in the model residuals (see *Sensitivity Analyses*, below).

Assessing the Impact of Island Isolation, Endemism, and Island Type.

Given the importance of the model and its parameters in island biogeography theory as outlined in the introduction, for the analyses described in this section, we focus exclusively on the log-power model (i.e., the linear model in log-log space). To explore the influence of island isolation and endemism on ISAR properties and residual variation, we took the following steps. First, we examined via partial linear regression (as e.g., ref. 49) the explanatory power of distance from mainland (log-transformed) in explaining residual variation from the global ISAR, also exploring how proportion of endemism is distributed in the same analyses. Partial regression (i.e., added-variable) plots were generated using the "avPlots" function in the "car" R package (50). Second, we assessed how the parameters of the log-power model (c -value, z -value, and R^2 value) varied across subsets of the data based on the proportion of SIEs (endemics) per island. In these analyses, we removed all islands with a proportion of SIEs less than (or equal to) 0.2% and fitted the log-power model to this subset of islands, storing the parameter values. This was then repeated using 0.5% SIEs as the threshold, and then using threshold values from 1% up to 25% in increments of 1%. We stopped at 25% to ensure there were enough islands within each group to undertake linear regression.

We also reran all models after restricting the selection to the oceanic islands (including both volcanic islands and atolls), that is, restricting the data to islands that have never been connected to or part of a larger mainland.

ASAR Model Fitting. We grouped islands into archipelagos, to fit the archipelago species-area relationship (ASAR) sensu Whittaker et al. (14). Using these archipelago data, we undertook the same species-area relationship model comparison outlined above, while also assessing the explanatory power of distance from mainland in explaining residual variation from the global ASAR. For ASARs, we present analyses for Archipelagic native species richness and for Archipelagic endemic species richness.

1. T. J. Matthews, K. A. Triantis, R. J. Whittaker, Eds., *The Species-Area Relationship: Theory and Application* (Cambridge University Press, Cambridge, 2021).
2. M. L. Rosenzweig, *Species Diversity in Space and Time* (Cambridge University Press, Cambridge, 1995).
3. I. S. Martins, H. M. Pereira, Improving extinction projections across scales and habitats using the countryside species-area relationship. *Sci. Rep.* **7**, 12899 (2017).
4. S. Fattorini, P. A. V. Borges, L. Dapporto, G. Strona, What can the parameters of the species-area relationship (SAR) tell us? Insights from Mediterranean islands. *J. Biogeogr.* **44**, 1018–1028 (2017).
5. C. Leclerc, C. Magneville, C. Bellard, Conservation hotspots of insular endemic mammalian diversity at risk of extinction across a multidimensional approach. *Divers. Distrib.* **28**, 2754–2764 (2021).
6. S. M. Scheiner, Six types of species-area curves. *Glob. Ecol. Biogeogr.* **12**, 441–447 (2003).
7. D. Storch, P. Keil, W. Jetz, Universal species-area and endemics-area relationships at continental scales. *Nature* **488**, 78–81 (2012).
8. K. A. Triantis, F. Guilhaumon, R. J. Whittaker, The island species-area relationship: Biology and statistics. *J. Biogeogr.* **39**, 215–231 (2012).
9. J. Schrader et al., Islands are key for protecting the world's plant endemism. *Nature* **634**, 868–874 (2024).
10. R. J. Whittaker, J.-M. Fernández-Palacios, T. J. Matthews, *Island Biogeography: Geo-Environmental Dynamics, Ecology, Evolution, Human Impact, and Conservation* (Oxford University Press, Oxford UK, 2023).
11. A. Kallmar, D. J. Currie, A global model of island biogeography. *Global Ecol. Biogeogr.* **15**, 72–81 (2006).
12. H. Kreft, W. Jetz, J. Mutke, G. Kier, W. Barthlott, Global diversity of island floras from a macroecological perspective. *Ecol. Lett.* **11**, 116–127 (2008).
13. R. H. MacArthur, E. O. Wilson, *The Theory of Island Biogeography* (Princeton University Press, Princeton, NJ, 1967).

Sensitivity Analyses. Given the spatial autocorrelation observed in the residuals of several of the models described above, and the known nonindependence of data points (islands) belonging to the same archipelago (51), we fitted alternative versions of the models to ensure our findings were robust to both spatial autocorrelation and archipelago-level effects. For the log-power ISAR model, we fitted both spatial autoregressive error models (52) and mixed-effects models (with archipelago included as a random intercept and slope [for both area and, where applicable, isolation]). These alternative models were fitted as part of both the all-island and oceanic island analyses, and also for the models including both area and isolation as predictors. For the ASAR analyses, we fitted only spatial autoregressive error models as an alternative, as the archipelago focus precluded the use of a mixed effect model with archipelago as a random effect. To further assess whether the effects of area and isolation were sensitive to the inclusion of additional standard covariates used in island biogeographic studies, we reran the previously described models, adding log-transformed elevation and absolute latitude as covariates.

For the semilog ISAR analysis, spatial autocorrelation was accounted for using a Bayesian Hierarchical Generalized Linear Mixed Model (negative binomial family) (53). The full details regarding the fitting and evaluations of these alternative models, including selecting the optimal spatial structure for the spatial autoregressive error models, is provided in the *SI Appendix*. All analyses were undertaken in R [v.4.3.2; (54)].

Data, Materials, and Software Availability. All code and data are available on GitHub (55). Other data are included in the article and/or supporting information.

ACKNOWLEDGMENTS. We thank the referees for their constructive criticism, and in particular Thomas J. Givnish for pointing out a conversion error in relation to the sizes of the continents in our first draft. H.K. acknowledges funding of research unit FOR2716 DynaCom (379417748) and Biodiversa+ BioMonI (533271599) from the German Research Foundation (DFG).

Author affiliations: ^aSchool of Geography, Earth and Environmental Sciences, University of Birmingham, Birmingham B15 2TT, United Kingdom; ^bBirmingham Institute of Forest Research, University of Birmingham, Birmingham B15 2TT, United Kingdom; ^cCentre for Ecology, Evolution and Environmental Changes/Azorean Biodiversity Group/Global Change and Sustainability Institute and Universidade dos Açores—Faculty of Agricultural Sciences and Environment, Angra do Heroísmo, Açores PT 9700-042, Portugal; ^dSchool of Natural Sciences, Macquarie University, Sydney, NSW 2109, Australia; ^eUniversité de Pau et des Pays de l'Adour, CNRS, Institut des Sciences Analytiques et de Physico-Chimie pour l'Environnement et les Matériaux, Pau 64000, France; ^fDepartment of Ecology and Taxonomy, Faculty of Biology, National and Kapodistrian University of Athens, Athens GR-15784, Greece; ^gDepartment of Biodiversity, Macroecology and Biogeography, University of Göttingen, Göttingen 37077, Germany; ^hDepartment of Environmental Science, Radboud Institute for Biological and Environmental Sciences, Radboud University, Nijmegen 6525AJ, The Netherlands; ⁱSchool of Geography and the Environment, and St Edmund Hall, University of Oxford, Oxford OX1 4AR, United Kingdom; and ^jCenter for Macroecology, Evolution and Climate, Globe Institute, University of Copenhagen, Copenhagen 1350, Denmark

14. R. J. Whittaker, J. M. Fernandez-Palacios, T. J. Matthews, M. K. Borregaard, K. A. Triantis, Island biogeography: Taking the long view of nature's laboratories. *Science* **357**, eaam8326 (2017).
15. M. V. Lomolino, Ecology's most general, yet protean pattern: The species-area relationship. *J. Biogeogr.* **27**, 17–26 (2000).
16. E. F. Connor, E. D. McCoy, The statistics and biology of the species-area relationship. *Am. Nat.* **113**, 791–833 (1979).
17. J. Schrader, Plants on small islands: Using taxonomic and functional diversity to unravel community assembly processes and the small-island effect. *Front. Biogeogr.* **12**, e47361 (2020).
18. T. J. Matthews et al., On the form of species-area relationships in habitat islands and true islands. *Glob. Ecol. Biogeogr.* **25**, 847–858 (2016).
19. T. J. Matthews, F. Rigal, K. A. Triantis, R. J. Whittaker, A global model of island species-area relationships. *Proc. Natl. Acad. Sci. U.S.A.* **116**, 12337–12342 (2019).
20. T. J. Matthews, K. A. Triantis, R. J. Whittaker, F. Guilhaumon, sars: An R package for fitting, evaluating and comparing species-area relationship models. *Ecography* **42**, 1446–1455 (2019).
21. K. A. Triantis, M. Mylonas, R. J. Whittaker, Evolutionary species-area curves as revealed by single-island endemics: Insights for the inter-provincial species-area relationship. *Ecography* **31**, 401–407 (2008).
22. K. A. Triantis, E. P. Economo, F. Guilhaumon, R. E. Ricklefs, Diversity regulation at macro-scales: Species richness on oceanic archipelagos. *Global Ecol. Biogeogr.* **24**, 594–605 (2015).
23. J. B. Losos, D. Schluter, Analysis of an evolutionary species-area relationship. *Nature* **408**, 847–850 (2000).
24. C. E. Wagner, L. J. Harmon, O. Seehausen, Cichlid species-area relationships are shaped by adaptive radiations that scale with area. *Ecol. Lett.* **17**, 583–592 (2014).
25. D. Schluter, M. W. Pennell, Speciation gradients and the distribution of biodiversity. *Nature* **546**, 48–55 (2017).
26. M. Williamson, K. J. Gaston, W. M. Lonsdale, The species-area relationship does not have an asymptote! *J. Biogeogr.* **28**, 827–830 (2001).

27. M. Williamson, K. J. Gaston, W. M. Lonsdale, An asymptote is an asymptote and not found in species-area relationships. *J. Biogeogr.* **29**, 1713–1713 (2002).
28. M. V. Lomolino, The species-area relationship: New challenges for an old pattern. *Prog. Phys. Geogr.* **25**, 1–21 (2016).
29. E. Munroe, "The size of island faunas" in *Proceedings of the Seventh Pacific Science Congress of the Pacific Sciences Association* (R. E. Owen Government printer, Wellington, New Zealand, 1953), vol. IV, pp. 52–53.
30. R. E. Ricklefs, I. J. Lovette, The roles of island area per se and habitat diversity in the species-area relationships of four Lesser Antillean faunal groups. *J. Anim. Ecol.* **68**, 1142–1160 (1999).
31. Y. Kisel, T. G. Barraclough, Speciation has a spatial scale that depends on levels of gene flow. *Am. Nat.* **175**, 316–334 (2010).
32. P. Ryan, E. de Juana, "Wilkins's finch (*Nesospiza wilkinsi*)" in *Birds of the World*, J. del Hoyo, A. Elliott, J. Sargatal, D. A. Christie, E. de Juana, Eds. (Cornell Lab of Ornithology, Ithaca, NY, USA, 2020).
33. L. Valente *et al.*, A simple dynamic model explains the diversity of island birds worldwide. *Nature* **579**, 92–96 (2020).
34. J. S. Cabral, P. Weigelt, W. D. Kissling, H. Kreft, Biogeographic, climatic and spatial drivers differentially affect alpha-, beta- and gamma-diversities on oceanic archipelagos. *Proc. Biol. Sci.* **281**, 20133246 (2014).
35. C. Rahbek *et al.*, Building mountain biodiversity: Geological and evolutionary processes. *Science* **365**, 1114–1119 (2019).
36. C. Rahbek *et al.*, Humboldt's enigma: What causes global patterns of mountain biodiversity? *Science* **365**, 1108–1113 (2019).
37. E. Marder, T. M. Smiley, B. J. Yanites, K. Kravitz, Direct effects of mountain uplift and topography on biodiversity. *Science* **387**, 1287–1291 (2025).
38. P. Weigelt, C. König, H. Kreft, GIFT-A global inventory of floras and traits for macroecology and biogeography. *J. Biogeogr.* **47**, 16–43 (2020).
39. R. Govaerts, E. N. Lughadha, N. Black, R. Turner, A. Paton, The world checklist of vascular plants, a continuously updated resource for exploring global plant diversity. *Sci. Data* **8**, 215 (2021).
40. C. Ulloa Ulloa *et al.*, An integrated assessment of the vascular plant species of the Americas. *Science* **358**, 1614–1617 (2017).
41. R. K. Brummitt, F. Pando, S. Hollis, N. Brummitt, "World geographical scheme for recording plant distributions Edition 2 (International working group on taxonomic databases for plant sciences)" (Hunt Institute for Botanical Documentation, Carnegie Mellon University, Pittsburgh, PA, 2001).
42. D. Hojsgaard, S. Klatt, R. Baier, J. G. Carman, E. Horandl, Taxonomy and biogeography of apomixis in angiosperms and associated biodiversity characteristics. *Crit. Rev. Plant Sci.* **33**, 414–427 (2014).
43. L. Cai *et al.*, Global models and predictions of plant diversity based on advanced machine learning techniques. *New Phytol.* **237**, 1432–1445 (2023).
44. L. Cai *et al.*, Climatic stability and geological history shape global centers of neo- and paleoendemism in seed plants. *Proc. Natl. Acad. Sci. U.S.A.* **120**, e2300981120 (2023).
45. T. J. Matthews, F. Rigal, Thresholds and the species-area relationship: A set of functions for fitting, evaluating and plotting a range of commonly used piecewise models in R. *Front. Biogeogr.* **13**, e49404 (2021).
46. K. P. Burnham, D. R. Anderson, *Model Selection and Multimodel Inference* (Springer, New York, ed. 2, 2002).
47. M. J. Brewer, A. Butler, S. L. Cooksley, R. Freckleton, The relative performance of AIC, AIC_c and BIC in the presence of unobserved heterogeneity. *Methods Ecol. Evol.* **7**, 679–692 (2016).
48. W. Venables, B. Ripley, W. Venables, *Modern Applied Statistics with S* (Springer, New York, 2002).
49. D. Lüdtke, M. Ben-Shachar, I. Patil, P. Waggoner, D. Makowski, Performance: An R package for assessment, comparison and testing of statistical models. *J. Open Source Softw.* **6**, 3139 (2021).
50. J. Fox, S. Weisberg, *An R Companion to Applied Regression* (Sage Publications, Los Angeles, 2018).
51. N. Bunnefeld, A. B. Phillimore, Island, archipelago and taxon effects: Mixed models as a means of dealing with the imperfect design of nature's experiments. *Ecography* **35**, 15–22 (2012).
52. E. Pebesma, R. Bivand, *Spatial Data Science: With Applications in R* (Chapman and Hall/CRC, Boca Raton, 2023).
53. S. C. Anderson, E. J. Ward, Black swans in space: Modeling spatiotemporal processes with extremes. *Ecology* **100**, e02403 (2019).
54. R Core Team, R: A language and environment for statistical computing (v.4.5.0, R Foundation for Statistical Computing, Vienna, Austria, 2025).
55. T. J. Matthews *et al.*, global_plant_ISAR. GitHub Repository. https://github.com/txm676/global_plant_ISAR. Deposited 4 January 2026.